Materials Research. 2017; 20(Suppl. 2): 447-451
DOI: http://dx.doi.org/10.1590/1980-5373-MR-2016-1081

Synthesis of the Perovskite-Type $BaCe_{0.8}Pr_{0.05}Cu_{0.15}O_{3-\delta}$ via EDTA-Citrate

Andarair Gomes dos Santos[a]*, Francisco Klebson Gomes dos Santos[a], Daniel Araujo de Macedo[b], Maxwell Ferreira Lobato[c], Ernani Dias da Silva Filho[d], Angélica Belchior Vital[e], Carlson Pereira de Souza[e]

[a]Departamento de Agrotecnologia e Ciências Sociais, Universidade Federal Rural do Semi-Árido - UFERSA, CEP: 59.625-900, Mossoró, RN, Brazil
[b]Departamento de Engenharia de Materiais, Universidade Federal da Paraíba, Campus I, Cidade Universitária, 58051-900, João Pessoa, PB, Brazil
[c]Centro de Ciências Exatas e Tecnologia, Universidade Federal do Maranhão, Av. dos Portugueses, 1966, Bacanga, 65080-805, São Luís, MA, Brazil
[d]Universidade do Estado do Rio Grande do Norte, Avenida Professor Antônio Campos, Presidente Costa e Silva, 59625620, Mossoró, RN, Brazil
[e]Departamento de Engenharia Química, Universidade Federal do Rio Grande do Norte - UFRN, 59.078-970, Natal, RN, Brazil

Received: December 13, 2016; Revised: April 07, 2017; Accepted: September 15, 2017

$BaCeO_3$-based ceramics are ionic and electronic conductors that can be applied to oxygen sensors, solid oxide fuel cells and oxygen permeable membranes. However, the low chemical stability at high temperatures of these materials motivates studies involving doping of A and/or B sites of the perovskite structure. In this context, the present work aimed to synthesize a new $BaCe_{0.8}Pr_{0.05}Cu_{0.15}O_{3-\delta}$ material using the chemical route of complexation which combines EDTA-Citrate with pH variation. The powders obtained at pH 3 or 11 and calcined up to 900 ºC are thermally unstable. The cubic perovskite $BaCe_{0.8}Pr_{0.05}Cu_{0.15}O_{3-\delta}$ with crystallite size between 99.4 nm and 131.6 nm was obtained along with barium carbonate traces. In the powders calcined at 1000 ºC the pH increase decreases the amount of barium carbonate (17.3% to pH 3, 3.4% to pH 7 and 1.8% to pH 11), but increases the size of grains with irregular shapes.

Keywords: *Perovskite, copper, $BaCe_{0.8}Pr_{0.05}Cu_{0.15}O_{3-\delta}$, EDTA-Citrate method*

1. Introduction

Interest in the perovskite type materials was motivated by its optical, electrical and magnetic properties[1,2]. Discovered in the 18th, the perovskite structure can be in its simple form (ABX_3)[3], yielding substituted compounds following the formula $A_xA'_xB_xB'_xO_3$[2,4] or in its complex form with structure $A_2B'B''O_6$[5], such as the compounds $BaLa(FeTi)O_6$[6] and $(A,Ba)Nb_2O_6$, with A = Sr, Na, K and Pb[7], which present great potential in optical computing and pyroelectric sensors.

The high catalytic activity of the perovskite type oxides (PTOs) allows these materials to be used in toluene degradation[8], carbon monoxide oxidation[9,10], biodiesel synthesis[11,12], solid oxide fuel cell cathode material[13-15], and as catalysts for methane reforming[16]. These and other applications and/or properties are derived from the specific characteristics of the perovskite type oxides, especially the ability to adsorb oxygen molecules (oxidation/reduction catalysts) and the presence of structural defects. These and other characteristics are directly related to the composition of the perovskite and its conditions of synthesis and processing. The composition and properties of the perovskites can be adjusted by simply doping A and/or B sites. The doping strategy affects the electronic state of the d-orbital, the stabilizing energy of the crystalline field and the binding energy B-O[17].

The effects of doping and synthesis method on the catalytic properties of perovskite-type oxides have been studied since 1950's. Perovskites with copper addition, more specifically the system La-Ba-Cu-O containing Cu^{2+} and Cu^{3+} have shown superconductivity at high temperatures[18]. In addition, one of the well-known properties of copper is its resistance to coke formation, avoiding catalytic deactivation. The presence of copper, even in small amounts, not only increases the resistance to carbon deposition, but also, in combination with Co element, increases the thermal stability of the compound[19].

The changes that occur in the atomic sites of the perovskite structure and the pH of the medium in which it is synthesized can cause changes in its structure and catalytic activity. In the present work, a perovskite of barium cerate doped with Pr and Cu ions of nominal composition $BaCe_{0.8}Pr_{0.05}Cu_{0.15}O_{3-\delta}$ was obtained by the complexation method combining EDTA-Citrate. Doping with praseodymium increases the content of oxygen vacancies, improving electrical properties[20]. At the same time, doping with copper improves the sinterability and transport properties in both air and hydrogen atmospheres[21]. The structure and morphology of the particulate materials

* e-mail: andarair@ufersa.edu.br.

were investigated as a function of the pH (basic, neutral or acid) of the reaction medium.

2. Experimental

The perovskite of composition $BaCe_{0.8}Pr_{0.05}Cu_{0.15}O_{3-\delta}$ was synthesized by the EDTA-citrate method[9,22,23] using the chemicals listed in Table 1.

During the synthesis, the pH of the solution ranged from 3 to 11. The experimental procedure was as follows: EDTA was diluted in ammonium hydroxide in the ratio 1 g:10 mL under constant stirring and controlled temperature (40 ºC). Then cations of sites A and B were added, keeping the stirring and temperature constant. Subsequently, citric acid was added and the temperature was raised to 80 ºC. The pH adjustment was done with the addition of ammonium hydroxide. The obtained gel was pre-calcined at 230 ºC using a heating rate of 5 ºC.min^{-1} for 180 min. The thermal behavior (TG) of the pre-calcined powder was analyzed in a Shimadzu equipment (DTG-60). Thermal analysis occurred in air atmosphere between room temperature and 900 ºC using a heating rate of 10 ºC min^{-1}. The structural characterization of calcined powders was performed by X-ray diffractometry (XRD) on a Bruker D2 Phaser diffractometer using Cu-Kα radiation (λ = 1.5406 Å) with Ni filter and Lynxeye detector. The measurements were made in a 2θ interval of 10º to 80º using current of 10 mA, voltage of 30 kV and scan rate of 0,01ºs^{-1}. The Rietveld refinement of the diffraction data was performed using the Maud software (version 2.55). The morphological analysis of powders was performed in a scanning electron microscope (SEM) of Hitachi (TM-3000) operated with incident electron beam of 15 kV. The chemical composition analysis was performed by X-Ray Fluorescence on a spectrometer with EDX – 720/800HS detector in a vacuum atmosphere.

3. Results and Discussion

Figure 1 shows mass loss curves of perovskite precursor powders $BaCe_{0.8}Pr_{0.05}Cu_{0.15}O_{3-\delta}$ synthesized at different pH values.

The powders presented the same thermal decomposition behavior up to 900 ºC, with no significant changes in mass

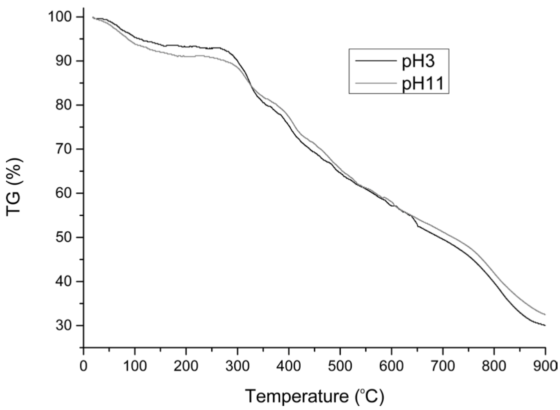

Figure 1. Thermogravimetric curves of precursor powders obtained in basic and acid pH.

loss with the pH change. It is possible to observe that the compound is not thermally stable in the analyzed temperature range, suggesting that calcination temperatures higher than 900 ºC should be used. However, in the temperature range analyzed, it can be verified that up to 900 ºC the stabilization process still does not occur, requiring a temperature above 900 ºC to obtain the phase. As the perovskite $BaCe_{0.2}Pr_{0.8}O_3$ was already obtained by EDTA-citrate followed by calcination at 1000 ºC[9], the powders obtained in the present work were calcined at 1000 ºC for 5 h.

Figure 2 shows the X-ray patterns of $BaCe_{0.8}Pr_{0.05}Cu_{0.15}O_{3-\delta}$ powders obtained with different pH values. It can be observed, regardless of the pH value (acid, neutral or basic), all powders present the barium cerate (79628-ICSD) and barium carbonate (15191-ICSD) phases. The phase quantification by Rietveld refinement indicated the presence of 1.8 wt%; 3.4 wt% and 17.3 wt% barium carbonate in powders synthesized at pH 11, 7 and 3, respectively. Considering the same calcination conditions, the structural characterization indicates that the purity of the synthesized material is affected by the pH of the reaction medium. The Rietveld refinement data (lattice parameters, crystallite sizes and weight fraction of each phase) and fitting parameters (R_{wp}, R_{exp} and χ^2; $\chi^2 = R_{wp}/R_{exp}$) are also listed in Table 2.

The chemical composition of powders was determined by X-ray dispersive energy, in order to identify the real

Table 1. Chemicals used in the synthesis of $BaCe_{0.8}Pr_{0.05}Cu_{0.15}O_{3-\delta}$ via EDTA-citrate.

Chemical	Molecular formula	Manufacturer	Purity (%)
EDTA acid	$C_{10}H_{16}N_2O_8$	Sigma/Aldrick	99.0
Barium nitrate	$Ba(NO_3)_2$	Sigma/Aldrick	99.0
Cerium nitrate	$Ce(NO_3)_3.6H_2O$	Sigma/Aldrick	99.4
Praseodymium nitrate	$Pr(NO_3)_3.6H_2O$	Sigma/Aldrick	99.0
Copper nitrate	$Cu(NO_3)_2.3H_2O$	Sigma/Aldrick	99.0
Citric acid	$C_6H_8O_7$	Sigma/Aldrick	99.5
Ammonium hydroxide	NH_4OH	Fluca	25

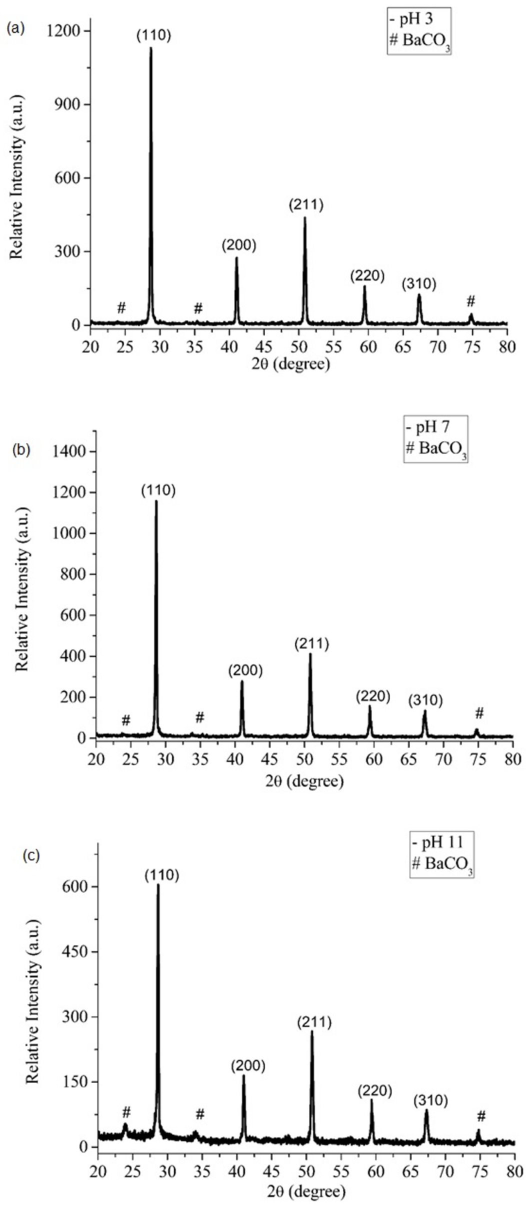

Figure 2. XRD patterns of $BaCe_{0.8}Pr_{0.05}Cu_{0.15}O_{3-\delta}$ powders synthesized with a different pH value after: a) pH 3, b) pH 7, c) pH 11.

stoichiometry of the perovskites. Tables 3 and 4 present the experimental values and experimental percentage errors, respectively, obtained for barium, cerium, praseodymium and copper elements.

Table 3. Chemical composition (expressed in wt%) of powders.

	Barium	Cerium	Praseodymium	Copper
pH	Experimental			
3	52.74	41.37	2.58	3.31
7	52.52	41.52	2.55	3.30
11	51.72	42.50	2.65	3.12

Table 4. Experimental errors (%) related to the chemical composition acquired by EDX.

pH	Erro (%)			
	Barium	Cerium	Praseodymium	Copper
3	2.39	1.83	2.64	7.60
7	1.96	1.47	3.77	7.82
11	0.41	0.85	0	12.74

It can be seen from Table 3 that, regardless of the pH, the experimental values obtained for the compound $BaCe_{0.8}Pr_{0.05}Cu_{0.15}O_{3-\delta}$ are close to the theoretical ones (51.51 wt% Ba, 42.14 wt% Ce, 2.65 wt% Pr and 3.58 wt% Cu). However, when the pH was basic, the percentage of copper presents the highest error%. Figure 3 shows SEM images of powders obtained with pH 3, 7 and 11. It can be observed that the powders consist of dense agglomerates, regardless of the pH value used. The powders obtained with pH 3 present small grains with irregular shapes (Figure 3 (B), whereas powders with pH 7 and 11 have more defined grains. The grain size increases with increasing pH value. Compared with samples of barium cerate without[19,24] and with doping ($BaCe_{0.2}Pr_{0.8}O_3$)[25], the powders obtained in this work present significant morphological changes. The perovskites $BaCeO_3$ and $BaCe_{0.2}Pr_{0.8}O_3$[7,24,25] showed a homogeneous distribution of particles and a fibrous-like shape, respectively. Such morphological changes are associated with the reduced

Table 2. Rietveld refinement data of $BaCe_{0.8}Pr_{0.05}Cu_{0.15}O_{3-\delta}$ powders obtained with different pH values and calcined at 1000 °C.

pH 3	pH 7	pH 11
χ^2= 1.09	χ^2= 1.22	χ^2= 1.00
Rwp (%) = 23.73	Rwp (%) = 28.15	Rwp (%) = 24.70
Rb (%) = 18.58	Rb (%) = 21.68	Rb (%) = 16.28
Rexp (%) = 21.62	Rexp (%) = 23.07	Rexp (%) = 24.57
a=b=c= 4.40 Å	a=b=c=4.40 Å	a=b=c=4.39 Å
TC=99.3 nm	TC=131.5 nm	TC=131.1 nm
Space group pm3m	Space group pm3m	Space group pm3m
Barium cerate(IV), weight	Barium cerate(IV), weight	Barium cerate(IV), weight
%: 82.71 +- 1.52	%: 96.59 +- 1.36	%: 98.23 +- 1.08
Barium carbonate , weight	Barium carbonate , weight	Barium carbonate , weight
%: 17.29 +- 2.61	%: 3.40 +- 0.38	%: 1.76 +- 0.23

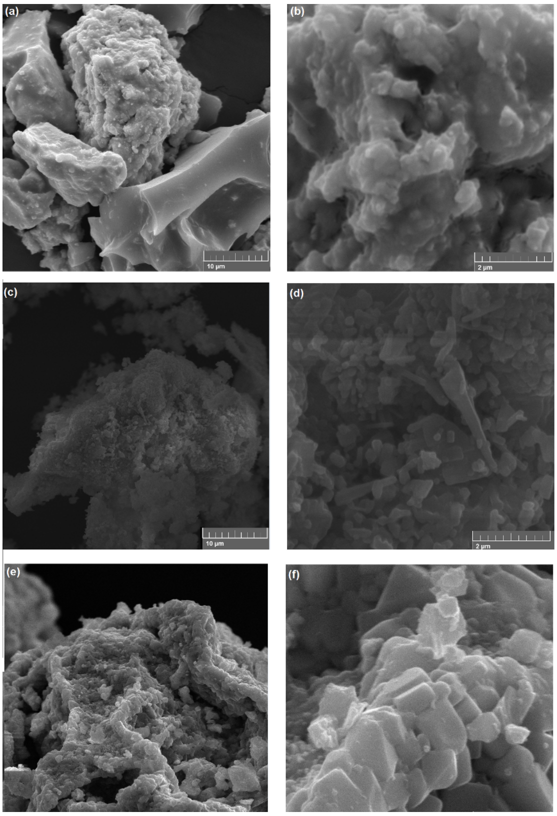

Figure 3. SEM images of $BaCe_{0.8}Pr_{0.05}Cu_{0.15}O_{3-\delta}$ powders, (A) and (B): pH 3, (C) and (D): pH 7, (E) and (F): pH 11.

calcination temperature range (900-950 ºC) and the absence of copper in the perovskite structure.

4. Conclusions

$BaCe_{0.8}Pr_{0.05}Cu_{0.15}O_{3-\delta}$ powders were obtained by the complexation method combining EDTA - Citrate. The barium carbonate content, a secondary phase common to all powders, decreased with increasing pH of the reaction medium, reaching a minimum of 1.8% for pH 11. The morphological characterization indicated the obtaining of dense agglomerates with grains of irregular shapes and increase in size with increasing the pH value.

5. Acknowledgments

The authors acknowledge CPVSA-UFERSA, LAMNRC-UFRN, and LAMOp-UERN.

6. References

1. Von Helmolt R, Wecker J, Holzapfel B, Schultz L, Samwer K. Giant negative magnetoresistance in perovskite-like $La_{2/3}Ba_{1/3}MnO_x$ ferromagnetic films. *Physical Review Letters* 1993;71(14):2331-2333.

2. Asai K, Yokokura O, Nishimori N, Chou H, Tranquada JM, Shirane G, et al. Neutron-scattermg study of the spin-state transition and magnetic correlations in $Lai_{1-x}.Sr_xCo0_3$ (x=0 and 0.08). *Physical Review B*. 1994;50(5):3025-3032.

3. Yamazoe N, Teraoka Y. Oxidation catalysis of perovskites --- relationships to bulk structure and composition (valency, defect, etc.). *Catalysis Today*. 1990;8(2):175-199.

4. Soares AB, Silva PRN, Freitas JCC, Almeida CM. Estudo da oxidação total do etanol usando óxidos tipo perovskita $LaBO_3$ (B= Mn, Ni, Fe). *Química Nova*. 2007;30(5):1061-1066.

5. Nakamura T. Monoclinic perovskite family of 1:1 ordered A2(B'B") O_6-compounds caused by g-type antiparallel displacements of a ions. *Materials Research Bulletin*. 1978;13(10):1023-1030.

6. Shankar U, Agarwal PK, Pandey R, Singh AK. Investigation of crystal structure of $SrLa(FeTi)O_6$ and $BaLa(FeTi)O_6$ perovskites by rietveld refinement. *Solid State Sciences*. 2016;52:78-82.

7. Moreno-Gobbi A, Paolini G, Pérez M, Negreira CA, Garcia D, Eiras JA. Caracterização ultra-sônica de materiais ferroelétricos com estrutura perovskita e tungstênio-bronze. *Cerâmica*. 2002;48(305):1-4.

8. Soltani T, Lee B. Improving heterogeneous photo-Fenton catalytic degradation of toluene under visible light irradiation through Ba-doping in $BiFeO_3$ nanoparticles. *Journal of Molecular Catalysis A: Chemical*. 2016;245:199-207.

9. Lobato MF, Santos AG, Vital AB, Souza CP. Síntese do cerato de bário pelo método de complexação combinando EDTA-citrato e avaliação catalítica na oxidação do monóxido de carbono testada em reator de leito fixo. *Cerâmica*. 2016;62(363):288-293.

10. Santos AG, Arab M, Patout L, Souza CP. $LaNi_{0.3}Co_{0.7}O_{3-\delta}$ and $SrFe_{0.2}Co_{0.8}O_{3-\delta}$ Ceramic Materials: Structural and Catalytic Reactivity under CO Stream. *Catalysts*. 2014;4(2):77-88.

11. Kesić Z, Lukić I, Zdujić M, Jovalekić C, Veljković V, Skala D. Assessment of $CaTiO_3$, $CaMnO_3$, $CaZrO_3$ and $Ca_2Fe_2O_5$ perovskites as heterogeneous base catalysts for biodiesel synthesis. *Fuel Processing Technology*. 2016;143:162-168.

12. Lima JRO, Ghani YA, Silva RB, Batista FMC, Bini RA, Varanda LC, et al. Strontium zirconate heterogeneous catalyst for biodiesel production: Synthesis, characterization and catalytic activity evaluation. *Applied Catalysis A: General*. 2012;445-446:76-82.

13. Meng F, Xia T, Wang J, Shi Z, Zhao H. Praseodymium-deficiency $Pr_{0.94}BaCo_2O_{6-\delta}$ double perovskite: A promising high performance cathode material for intermediate-temperature solid oxide fuel cells. *Journal of Power Sources*. 2015;293:741-750.

14. Kong X, Zhou X, Tian Y, Wu X, Zhang J, Zuo W, et al. Efficient and stable iron based perovskite $La_{0.9}Ca_{0.1}Fe_{0.9}Nb_{0.1}O_{3-\delta}$ anode material for solid oxide fuel cells. *Journal of Power Sources*. 2016;316:224-231.

15. Jin F, Liu J, Niu B, Ta L, Li R, Wang Y, et al. Evaluation and performance optimization of double-perovskite $LaSrCoTiO_{5+\delta}$ cathode for intermediate-temperature solid-oxide fuel cells. *International Journal of Hydrogen Energy*. 2016;41(46):21439-21449.

16. Barros BS, Kulesza J, Melo DMA, Kienneman A. Nickel-based Catalyst Precursor Prepared Via Microwave-induced Combustion Method: Thermodynamics of Synthesis and Performance in Dry Reforming of CH_4. *Materials Research*. 2015;18(4):732-739.

17. Toniolo FS. *Óxidos mistos do tipo perovskita para a geração de gás de síntese* [Tese]. Rio de Janeiro: Universidade Federal do Rio de Janeiro; 2010.

18. Yuan CC, Wu DS, Wang CM, Kao HCI. Superconductivity of $La_{1.5-x2}Sr_xBa_{1.5-x2}Cu_3O_y$ compounds. *Physica C: Superconductivity*. 1996;268(1-2):128-132.

19. Lee S, Ahn K, Vohs JM, Gorte RJ. Cu-Co Bimetallic Anodes for Direct Utilization of Methane in SOFCs. *Electrochemical and Solid-State Letters*. 2005;8(1):A48-A51.

20. Neeraj K, Panwar N, Gahtori B, Singh N, Kishan H, Awana VPS. Structural, dielectric and magnetic properties of Pr substituted $Bi_{1-x}Pr_xFeO_3$ ($0 \leq x \leq 0.15$) multiferroic compounds. *Journal of Alloys and Compounds*. 2010;501(9):29-32.

21. Gorbova E, Maragou V, Medvedev D, Demin A, Tsiakaras P. Influence of Cu on the properties of gadolinium-doped barium cerate. *Journal of Power Sources*. 2008;181(2):292-296.

22. Santos AG, Silva RR, Dantas AGO, Lobato MF, Souza CP. Efeito do pH, Razão molar de EDTA: Ácido cítrico: íons metálicos totais e do tratamento térmico na obtenção da $BaCeO_3$ com base no método de complexação EDTA-Citrato. *Revista Verde*. 2014;9(4):149-162.

23. Santos AG, Costa IKF, Santos FKG, Souza CP. Efeito do método de complexação combinando EDTA - Citrato e coprecipitação em meio oxalato na síntese da $SrCo_{0,8}Fe_{0,2}O_3$. *HOLOS*. 2014;3:30-43.

24. Lopes FWB, Arab M, Macedo HP, Souza CP, Sousa JF, Gavarri JR. High temperature conduction and methane conversion capability of $BaCeO_3$ perovskite. *Powder Technology*. 2012;219;186-192.

25. Lobato MF, Souza CP, Passos RH, Santos AG, Gomes IRB. Efeito da variação de pH na síntese e nas propriedades de $BaCe_{0,2}Pr_{0,8}O_3$ obtido pelo método de complexação EDTA-Citrato. *Cerâmica*. 2014;60:532-536.